Acta Pharmaceutica Sinica B 2025;15(10):5022−5035

Chinese Pharmaceutical Association
Institute of Materia Medica, Chinese Academy of Medical Sciences

Acta Pharmaceutica Sinica B

www.elsevier.com/locate/apsb
www.sciencedirect.com

ORIGINAL ARTICLE

A preclinical and first-in-human study of superstable homogeneous radiolipiodol for revolutionizing interventional diagnosis and treatment of hepatocellular carcinoma

Hu Chen[a,b,†], Yongfu Xiong[c,†], Minglei Teng[a,g,†], Yesen Li[e,†], Deliang Zhang[h], Yongjun Ren[c], Zheng Li[c], Hui Liu[a], Xiaofei Wen[e], Zhenjie Li[a,i], Yang Zhang[a], Syed Faheem Askari Rizvi[a,j], Rongqiang Zhuang[a], Jinxiong Huang[e], Suping Li[c,*], Jingsong Mao[f,*], Hongwei Cheng[a,d,*], Gang Liu[a,*]

[a]*State Key Laboratory of Infectious Disease Vaccine Development, Xiang An Biomedicine Laboratory, National Innovation Platform for Industry-Education Integration in Vaccine Research, Fujian Engineering Research Center of Molecular Theranostic Technology, Center for Molecular Imaging and Translational Medicine, School of Public Health, Xiamen University, Xiamen 361102, China*
[b]*Shaanxi Province Center for Regenerative Medicine and Surgery Engineering Research, the First Affiliated Hospital of Xi'an Jiaotong University, Xi'an 710061, China*
[c]*Department of Hepatobiliary Surgery, Department of Nuclear Medicine, Academician (Expert) Workstation, Sichuan Digestive System Disease Clinical Medical Research Center, Affiliated Hospital of North Sichuan Medical College, Nanchong 637000, China*
[d]*Zhuhai UM Science & Technology Research Institute, University of Macau, Macau 999078, China*
[e]*Department of Nuclear Medicine, Department of Vascular & Tumor Interventional Radiology, the First Affiliated Hospital of Xiamen University, School of Medicine, Xiamen University, Xiamen 361003, China*
[f]*Department of Interventional Vascular Surgery, the Sixth School of Clinical Medicine, the Affiliated Qingyuan Hospital (Qingyuan People's Hospital), Guangzhou Medical University, Qingyuan 511518, China*
[g]*School of Biomedical Engineering, Shanghai Jiao Tong University, Shanghai 200030, China*
[h]*Department of Nuclear Medicine, the Xiang'an Affiliated Hospital of Xiamen University, Xiamen 361102, China*

This article is part of a special issue entitled: Targeted Radiopharmaceuticals published in Acta Pharmaceutica Sinica B.

*Corresponding authors.
E-mail address: gangliu.cmitm@xmu.edu.cn (Gang Liu), zumri.hwcheng@um.edu.mo (Hongwei Cheng), maojingsong163@163.com (Jingsong Mao), li807635272@163.com (Suping Li).
[†]These authors made equal contributions to this work.

Peer review under the responsibility of Chinese Pharmaceutical Association and Institute of Materia Medica, Chinese Academy of Medical Sciences.

https://doi.org/10.1016/j.apsb.2025.02.021

[i]*Department of Radiation Oncology, Peking University Shenzhen Hospital, Shenzhen 518000, China*
[j]*Institute of Molecular Biology and Biotechnology (IMBB), the University of Lahore, Lahore 54000, Pakistan*

Received 1 December 2024; received in revised form 17 January 2025; accepted 18 January 2025

KEY WORDS

Hepatocellular carcinoma;
Intravascular intervention;
Radionuclide;
Lipiodol;
Superstable homogeneous iodinated formulation technology;
Nuclear medicine imaging;
Transarterial radioembolization;
Theranostics

Abstract Transarterial radioembolization (TARE) is a widely utilized therapeutic approach for hepatocellular carcinoma (HCC), however, the clinical implementation is constrained by the stringent preparation conditions of radioembolization agents. Herein, we incorporated the superstable homogeneous iodinated formulation technology (SHIFT), simultaneously utilizing an enhanced solvent form in a carbon dioxide supercritical fluid environment, to encapsulate radionuclides (such as ^{131}I,^{177}Lu, or ^{18}F) with lipiodol for the preparation of radiolipiodol. The resulting radiolipiodol exhibited exceptional stability and ultra-high labeling efficiency (≥99%) and displayed notable intratumoral radionuclide retention and *in vivo* stability more than 2 weeks following locoregional injection in subcutaneous tumors in mice and orthotopic liver tumors in rats and rabbits. Given these encouraging findings, ^{18}F was authorized as a radiotracer in radiolipiodol for clinical trials in HCC patients, and showed a favorable tumor accumulation, with a tumor-to-liver uptake ratio of ≥50 and minimal radionuclide leakage, confirming the feasibility of SHIFT for TARE applications. In the context of transforming from preclinical to clinical screening, the preparation of radiolipiodol by SHIFT represents an innovative physical strategy for radionuclide encapsulation. Hence, this work offers a reliable and efficient approach for TARE in HCC, showing considerable promise for clinical application (ChiCTR2400087731).

1. Introduction

Hepatocellular carcinoma (HCC) is one of the leading causes of cancer-related death worldwide, and its incidence and mortality rates are increasing annually[1]. Patients in the intermediate and advanced stages are subjected to passive treatments due to the insufficient diagnosis of early symptoms[2]. Therefore, early accurate diagnosis and effective administration strategies are essential for improving the survival rates of HCC patients. Radionuclide-based therapies have gained prominence in cancer theranostics, offering diagnostic imaging and targeted radiotherapy[3,4]. Transarterial radioembolization (TARE) represents a minimally invasive and effective locoregional treatment approach for unresectable HCC, demonstrating a notable ability to inhibit tumor progression while minimizing side effects[5]. TARE involves delivering radionuclide-labeled agents that irradiate tumor cells *via* α/β emissions through endovascular intervention. Effective radionuclide internal radiotherapy for HCC requires high-labeling-efficiency carriers that specifically accumulate and remain stable in tumors[6]. Numerous radioembolic agents such as ^{90}Y microspheres[7], ^{166}Ho microspheres[8], ^{177}Lu microspheres[9,10], ^{131}I microspheres[11], radiolipiodol have been developed and investigated for HCC[12]. However, complicated preparation methods for radioembolic agents restrict the wide clinical application of TARE[13-15].

Lipiodol is commonly used as a carrier in transcatheter arterial chemoembolization (TACE) due to its ability to selectively deposit in hypervascularized liver tumors[16]. ^{131}I-encapsulated radiolipiodol formulation (^{131}I-LUF) was introduced for TARE, combining the embolic properties of lipiodol with the therapeutic effects of radionuclides[17]. Despite the initial success, the preparation of ^{131}I-LUF required higher temperatures, resulting in the volatilization and oxidation of iodine. This compromised formulation stability and posed a risk of adverse effects, such as radiation pneumonitis, resulting from unintended distribution[18,19]. In addition, the physical emulsification method for preparing radiolipiodol exhibited instability, leading to rapid stratification and radionuclide leakage, which diminished the therapeutic efficacy and increased systemic radiation exposure[20]. Consequently, improving the preparation methods for radiolipiodol is expected to expand the application of TARE in HCC.

To address these challenges faced in the production of radiolipiodol, this study explores the application of superstable homogeneous iodinated formulation technology (SHIFT) to improve the manufacturing process of radiolipiodol. SHIFT utilizes the unique solvent properties of carbon dioxide (CO_2) in a supercritical fluid (SCF) environment, which allows for precise control over temperature and pressure to modify key parameters, including the density, diffusion coefficient, and viscosity of lipiodol[21]. This method significantly improves the dispersion of solutes, facilitating more uniform and stable encapsulation, while maintaining the inherent properties of the encapsulated agents and eliminating the need for emulsifiers[22]. Our research team has previously explored the effective implementation of SHIFT and the incorporation of photosensitizers and chemotherapeutic agents into lipiodol, demonstrating improved stability and therapeutic outcomes in HCC treatments[23-26]. Herein, we expanded on our prior work by rigorously investigating the preparation of various radiolipiodol formulations using SHIFT, including ^{131}I-LUF, ^{18}F-

encapsulated lipiodol (^{18}F-LUF), and ^{177}Lu-encapsulated lipiodol (^{177}Lu-LUF). We systematically evaluated the feasibility of this strategy for TARE-based diagnosis and treatment of HCC (Scheme 1). As proof of concept, the obtained radiolipiodol formulations exhibited superior stability and encapsulation efficiencies exceeding 99%, with radionuclide release rates as low as 5%, significantly lower than those of conventional mixtures over similar periods. Furthermore, preclinical studies in mouse, rat, and rabbit HCC tumor models demonstrated good intratumoral radionuclide retention and minimal leakage of the SHIFT-empowered radiolipiodol, which were confirmed by clinical trials in HCC patients. In conclusion, the preparation of radiolipiodol *via* SHIFT presents notable advantages over conventional radionuclide labeling methods, effectively overcoming many of the inherent limitations associated with radionuclides. This innovative approach holds great potential to redefine and improve TARE-based diagnostic and therapeutic strategies for HCC, providing a new paradigm for the treatment of this challenging malignancy.

2. Materials and methods

2.1. Materials

Fetal bovine serum (FBS) and high glucose Dulbecco's modified Eagle medium (DMEM) culture medium were purchased from Hyclone Co., Ltd. (Logan, Utah, USA); antibiotics (double antibodies for culture medium) were obtained from Shenggong Biotechnology Co., Ltd. (Shanghai, China); high-efficiency thin layer chromatography silica gel plates were purchased from Acmec Biochemical Co., Ltd. (Shanghai, China); gadobutrol contrast agent was acquired from Bayer Co., Ltd. (Leverkusen, Germany); Zoletil anesthesia for veterinary use was purchased from Shengda Animal Pharmaceutical Co., Ltd. (Jilin, China); Lipiodol and iohexol were purchased from Jiangsu Hengrui Medicine Co., Ltd. (Lianyungang, China); heparin sodium was acquired from National Pharmaceutical Group Chemical Reagent Co., Ltd. (Shanghai, China); povidone-iodine disinfectant solution was purchased from Shandong Lilkang Co., Ltd. (Jinan, China).

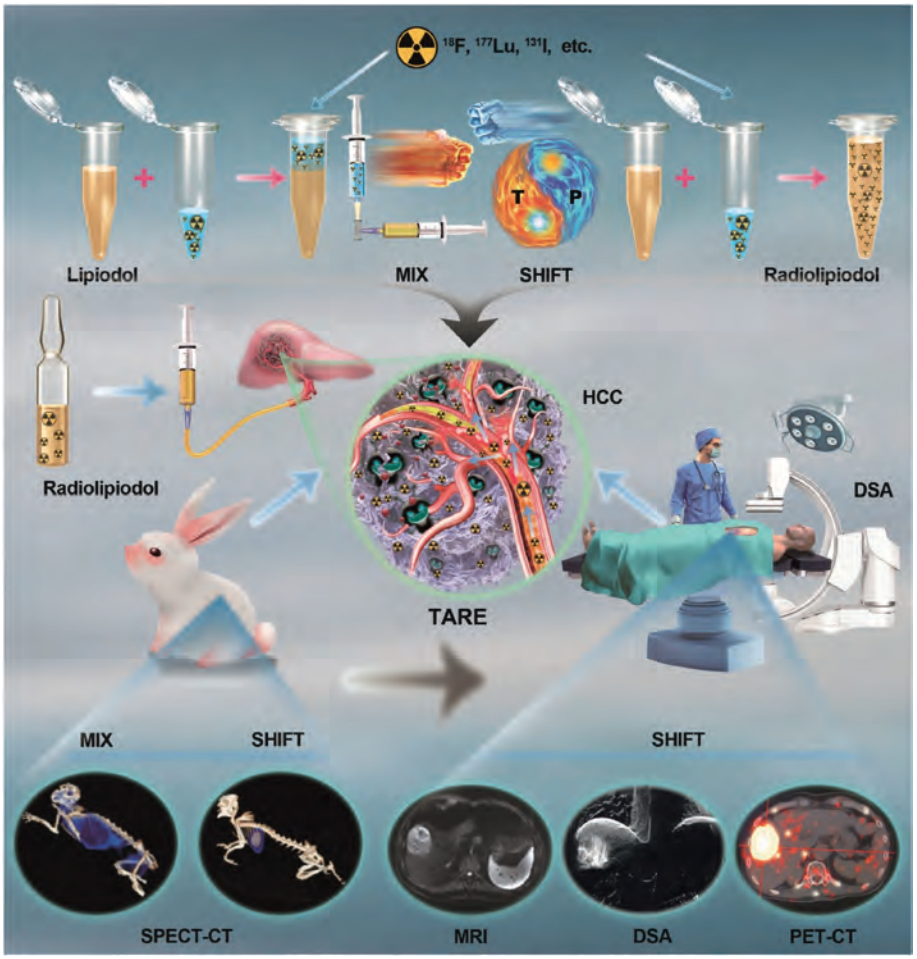

Scheme 1 Schematic illustration of superstable homogeneous radiolipiodol for the interventional diagnosis and treatment of HCC. Radiolipiodol, comprising various radionuclides (^{18}F,^{177}Lu, or ^{131}I) and embolic agent lipiodol, was initially prepared by traditional three-way syringe mixing (MIX) and SHIFT. SHIFT-empowered radiolipiodol is homogeneous and stable, in contrast to Radiolipiodol (MIX), which stratified because of instability. After intra-arterial injection of radiolipiodol into the liver tumor on rabbit, the diffusion of radiolipiodol (MIX) and the stable accumulation of radiolipiodol (SHIFT) *in vivo* were confirmed by imaging. Furthermore, remarkable accumulation of radiolipiodol (SHIFT) in tumors of HCC patients by interventional method in clinical practice was validated, showing promising diagnostic value for HCC.

$^{177}LuCl_3$ was obtained from Xinke Pharmaceuticals Co., Ltd. (Chengdu, China); Anhydrous ethanol and sodium citrate were purchased from Sigma−Aldrich Biochemical Technology Co., Ltd. (Shanghai, China); $Na^{131}I$ was provided by Atomic High-Tech Co., Ltd. (Beijing, China). $Na^{18}F$ and $^{64}CuCl_2$ are produced by the Center of Molecular Imaging and Translational Medicine, Xiamen University (Xiamen, China).

2.2. Cell lines and experimental animals

H22 mouse liver cancer cells were purchased from the American Type Culture Collection (ATCC, Manassas, VA, USA). N1−S1 rat liver cancer cells were donated by Lishui Hospital of Zhejiang University and also purchased from ATCC. VX2 tumor blocks were purchased from Lailan Biotechnology Co., Ltd. (Shanghai, China). Balb/c mice (16−18 g), SD rats (120−150 g), and New Zealand white rabbits (2.5−3.0 kg) were bought from Slake Experimental Animals Co., Ltd. (Shanghai, China) and used as per guidelines approved from the Animal Care and Use Committee of Xiamen University (ACUCXU).

2.3. Preparation of radiolipiodol

Initially, 5 mCi of radionuclides were diluted with 50−500 μL of absolute ethanol and then they were subsequently added to 5 mL of lipiodol, followed by ultrasonic vibration and dispersion for 10 min. The resulting mixture was transferred to the reaction vessel of a SHIFT instrument. After securing the reaction vessel, CO_2 gas was pressurized to 15 MPa and heated to 37 °C, resulting in a supercritical fluid state of CO_2. The reaction was performed for 30−120 min at a stirring speed of 800 rpm. Subsequently, the mixture was allowed to stand for 30 min, after which the sample within the reactor was collected to obtain superstable radiolipiodol. The radionuclide concentrations before and after the reaction were quantified using an activity meter.

2.4. In vitro studies of radiolipiodol

The labeling efficiency of radiolipiodol was measured by thin-layer chromatography (TLC) analysis using a Mini-Scan TLC scanner (BioScan, Washington DC, USA). Saline and 1 mmol/L sodium citrate were used as the expanding agents for TCL of ^{131}I and ^{177}Lu, respectively. The radiolipiodol was dispensed in 1.5 mL centrifuge tubes and imaged with the use of a SPECT imaging system (Mediso nanoScan, Budapest, Hungary) to visualize the distribution of radionuclides in the lipiodol. Saline was used as the extraction solution, thus, the upper extraction solution in the mixture of saline and radiolipiodol was sucked at 1, 2, 4, 8, 12, and 24 h, and the radioactivity was measured synchronously with the reserved 1% of the sample using a γ counter (PerkinElmer WIZARD2 2480, Waltham, MA, USA). The MPC value was obtained to evaluate the *in vitro* release behavior of radionuclides. The calculation formula is as shown in Eq. (1):

$$\text{Release rate (\%)} = (\text{MPC (1\% upper fluid)} / \text{MPC (1\% radiolipiodol)}) \times 100 \quad (1)$$

The Cerenkov luminescence detection of ^{18}F radionuclide with an activity of 100 μCi/mL was performed using the IVIS Living Image System (Caliper IVIS Lumina II, Hopkinton, MA, USA).

2.5. Construction of the animal model

The mouse hepatoma H22 cells were resuspended in PBS to 5×10^6/100 μL, and then the cell suspension was injected subcutaneously into the hind legs of BALB/c mice. When the tumor palpation started in a week and its size reached about 100 mm^3, 50 μL of radiolipiodol containing 20 μCi radionuclide was injected into the tumor of mice using an insulin needle for *in vivo* study. Similarly, the rat hepatoma N1−S1 cells were resuspended in PBS to 5×10^6/100 μL for later use. SD rats weighing 120−150 g were anesthetized, and their livers were exposed by laparotomy, and 100 μL of cell suspension was injected into the liver parenchyma using an insulin needle. Rats were scanned using a 9.4 T magnetic resonance imaging (MRI) system (Bruker 9.4 T MicroMRI, Billerica, MA, USA) with a T2 sequence to check for orthotopic HCC growth. Intra-arterial drug injection was performed when the tumor was approximately 50 mm^3 in size. After anesthesia, the abdomen of the tumor-bearing rats was opened, and approximately 75 μL of radiolipiodol containing 50 μCi radionuclide was injected slowly in the direction of the proper hepatic artery by inserting an insulin needle backward into the duodenal artery. After injection of the formulations, the duodenal artery was ligated, the wound was sutured, and the recovery as well as survival status of the rats were observed. Furthermore, the New Zealand white rabbits (2.5−3.0 kg) were anesthetized, and the needle was introduced into the liver under ultrasound guidance. The prepared VX2 rabbit tumor mass was delivered into the liver by trocar. The growth of the tumor was observed by a 3.0 T MRI system (Siemens MAGNETOM Skyra 3T, Berlin, Germany), and the size of the tumor was allowed to grow up to about 600−1000 mm^3 before the interventional injection of radiolipiodol. The interventional injection was performed under the guidance of a digital subtraction angiography (DSA) system (Siemens Artis zeegoIII, Berlin, Germany). After anesthesia of the tumor-bearing rabbits, the muscle tissue was isolated, and the femoral artery was exposed by blunt separation using hemostatic forceps. An 18G trocar puncture needle was inserted into the femoral artery and a 5-F vascular sheath was introduced. Under real-time DSA guidance, the microguidewire guided the microcatheter through the vascular sheath to the nearest artery of the tumor blood supply. Approximately 200 μL of radiolipiodol containing 50 μCi radionuclide was slowly injected through the microcatheter using a 1 mL syringe after the microguidewire was pulled out. DSA visualization demonstrated that radiolipiodol successfully reached the vascular supply and subsequently accumulated within the tumor region.

2.6. In vivo imaging study

The distribution of radiolipiodol in the tumor-bearing mice and rats was observed *via* small animal SPECT-CT imaging system (Mediso) at 1, 24, 72, and 168 h post-radiolipiodol injection. For rabbits, SPECT-CT imaging (GE Discovery NM/CT 670 Pro, Boston, MA, USA) and PET-CT imaging (GE Discovery MI Gen 2, Boston, MA, USA) systems were utilized following the injections of radiolipiodol containing either ^{177}Lu, ^{131}I, or ^{18}F, and the signal changes in the tumor area and normal tissues were observed and counted.

2.7. Blood metabolic analysis

For the blood metabolism test, approximately 10 μL of venous blood was collected at 2, 4, 8, 12, 24, 72, and 168 h post-injection

of radiolipiodol. The blood of mice and rats was collected from the tip of the tail, and the blood of rabbits was collected from the ear vein. MPC values were obtained by synchronously measuring the blood and 1% radiolipiodol of the reserved injection dose using an γ counter (PerkinElmer). The content of radionuclide in blood was calculated using Eq. (2):

$$\%\ \text{injected dose per gram (\%ID/g)} = \text{MPC (blood)} / \text{weight} / \text{MPC (1\% injection dose)} \quad (2)$$

2.8. Biodistribution study

Various organs such as the heart, liver, spleen, lung, kidney, intestine, stomach, tumor tissue, and other tissues were collected and weighed after the experimental animals were sacrificed on the seventh-day post-injection of radiolipiodol. The collected tissue was then synchronized with 1% radiolipiodol of the reserved injection dose for radioactivity measurement using an γ counter (PerkinElmer) to obtain MPC values. The biodistribution of the radionuclides in tumor and organ tissues was calculated using Eq. (3):

$$\%\text{ID/g} = \text{MPC (organ tissue)} / \text{weight} / \text{MPC (1\% injection dose)} \quad (3)$$

The ratio between tumor and normal tissues was calculated using Eq. (4):

$$\text{Ratio}(T/N) = \%\text{ID/g (tumor)} / \%\text{ID/g (organ tissue)} \quad (4)$$

2.9. Clinical trials in HCC

The clinical trial received approval from the Ethics Committee of the Affiliated Hospital of North Sichuan Medical College (approval numbers: 2022ER505-1, 2024ER390-1) and has been registered with the Chinese Clinical Trial Registry (registration number: ChiCTR2400087731). After the identification of suitable subjects, the SHIFT instrument was transported to the nuclear medicine department of the Affiliated Hospital of North Sichuan Medical College (Supporting Information Fig. S1A). By aseptic principles, the preparation of ^{18}F-LUF was conducted following the aforementioned method. Subsequently, it was combined with conventional chemotherapeutic agents as required to exert its therapeutic effects (Fig. S1B). For injecting the formulations, the femoral artery was punctured, and DSA was utilized to image the celiac trunk and superior mesenteric artery to identify the tumor's feeding artery. Subsequently, a microcatheter was superselected into the identified feeding artery, and an appropriate amount of a radioactive adriamycin and radiolipiodol mixture was administered. The dosage was determined based on the tumor size, generally not exceeding 20 mL, with the radionuclide dose approximately within 1 mCi. Embolization ceased once the blood flow within the target artery became stagnant, or reflux was observed.

As for postoperative management, the patient was supine for 24 h and the puncture site was pressurized with sandbags for 6 h. All patients were treated with liver-protective, stomato-protective, symptomatic, and supportive treatments. Blood routine, coagulation, liver and kidney function were rechecked every other day to evaluate the adverse reactions such as myelosuppression after surgery, and antibiotics were given if necessary. Sophisticated timely pay attention to the possible adverse reactions of interventional surgery and iodine allergic reaction, if there were any symptomatic treatment effects observed in time.

The patients were promptly transferred to the Nuclear Medicine Department for PET-CT scanning (GE Discovery 710, Boston, MA, USA) immediately following surgery. Imaging data were acquired at 30 min and 180 min postoperatively to assess the distribution of radionuclides within the body (Fig. S1C). Throughout the examination, patients' vital signs, including heart rate, respiration, and blood pressure, were continuously monitored. Additionally, patients were queried regarding any adverse reactions after the procedure. Post-administration observation and precautionary measures were implemented by the hospital's established radiopharmaceutical safety protocols.

2.10. Statistical analysis

Data are shown as mean $\pm$ standard error of mean (SEM). The statistical methods used include Student's *t*-test for the comparison of two groups and two-way ANOVA for the comparison between multiple groups. Graphs were plotted by GraphPad Prism 8.0 software (GraphPad, Boston, MA, USA). $^{*}P < 0.05$, $^{**}P < 0.01$, $^{***}P < 0.001$ were considered as significant statistical differences.

3. Results

3.1. In vitro stability of radiolipiodol

Radiolabeling of lipiodol *via* the isotope replacement method under high-temperature reaction conditions results in the free participation of iodine to interact with lipiodol and change its viscosity, which can affect embolization and angiography performance[27]. Lipiodol has superior solubility which can significantly improve the dispersibility of solutes in mild CO_2 SCF environment[28]. We prepared radiolipiodol by using SHIFT to optimize the traditional chemical labeling method of radionuclides (Fig. 1A). In short, the radionuclide was first dispersed in a trace amount of solvent and further dispersed in lipiodol. The above mixture was added to the reaction kettle of superstable homogeneous mixing instrument, and stable radiolipiodol (named LUF(S)) can be obtained after the end of the reaction in the CO_2 SCF fluid state. Supercritical fluids serve as environmentally friendly solvents, functioning under mild conditions and demonstrating high diffusivity alongside low viscosity[22]. The characteristics promote rapid mass transfer, allowing for efficient dissolution and loading of radionuclides into lipiodol. This method addresses the limitations of traditional heterogeneous mixing and circumvents the challenges related to elevated temperatures or strong acids commonly found in conventional radionuclide drug preparation techniques. This advancement significantly enhances the radiotherapeutic efficacy and stability of radiolipiodol. The yield of radiolipiodol under different conditions was explored at first. After the reaction time, maintenance temperature, rotational speed, system pressure, and other basic parameters were fixed according to the previous experimental experience, further, the optimal production conditions such as the feeding ratio and the amount of solvent were also determined. As shown in Supporting Information Table S1, when preparing ^{131}I-LUF with a solvent volume ranging from 0.1 to 0.2 mL and the input ratio of lipiodol to ^{131}I is 4 mL to 3 mCi, resulting in a radionuclide recovery yield between 55% and 70% and a specific

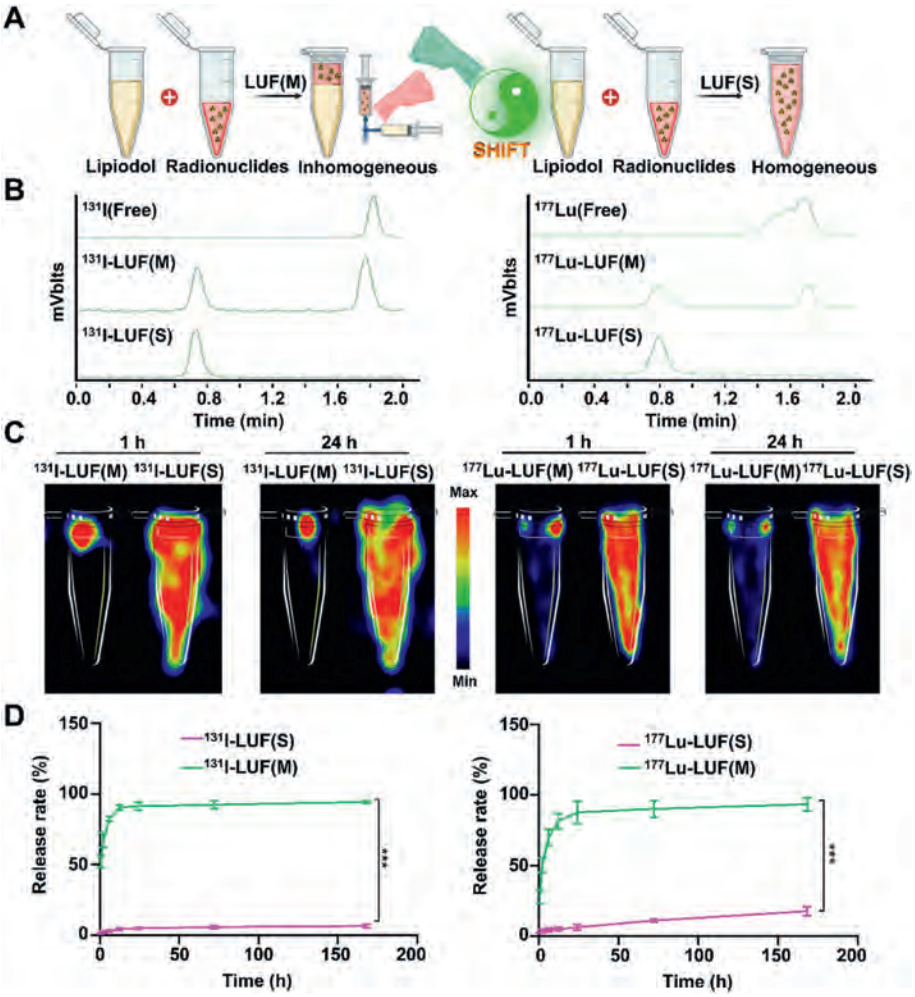

Figure 1 The construction and characterization of SHIFT-assisted superstable homogenous radiolipiodol. (A) Schematic illustration of the superstable homogeneous radiolipiodol by SHIFT, overcoming the inhomogeneous features caused by traditional mixing method. (B) TLC curve of a free radionuclides solution, LUF(M) and LUF(S), including ^{131}I (left panel) and ^{177}Lu (right panel). (C) Following the preparation of radiolipiodol from the common mixing group and the SHIFT preparation group, SPECT scanning of ^{131}I-LUF and ^{177}Lu-LUF was conducted at 1 and 24 h post-preparation, respectively. (D) Release profile of ^{131}I and ^{177}Lu from ^{131}I-LUF and ^{177}Lu-LUF, respectively. Data are presented as mean ± SD ($n = 3$). ***$P < 0.001$ were considered as significant statistical differences.

activity of approximately 0.65 mCi/mL. Upon substituting preparation of ^{177}Lu-LUF with absolute ethanol as solvent, exceeding 60% of the recovery rate of the radionuclide at the input ratio of lipiodol to ^{177}Lu is 1 mL to 1 mCi. Additionally, the specific activity achieved was 0.7 mCi/mL.

The stability of radiolipiodol is crucial for its effective *in vivo* applications. To assess the encapsulating efficiency of radiolipiodol, TLC experiments were conducted, among free radionuclides, and hand-mixed radiolipiodol (named LUF(M)) was used as a control. As shown in Fig. 1B and Supporting Information Figs. S2A and a single peak at approximately 0.7 min in the spectra of both ^{131}I-LUF(S) and ^{177}Lu-LUF(S) indicates minimal abscission of ^{131}I, ^{177}Lu, and ^{18}F in lipiodol, with an encapsulating efficiency exceeding 99%. Additionally, SPECT imaging was employed to visually observe the distribution of radionuclides in lipiodol leveraging the imaging properties of the radionuclides (Fig. 1C and Fig. S2B). In the SPECT image, a bright signal is observed on the surface of radiolipiodol prepared by a simple mixture, validating the radionuclides rapidly stratified and gathered above the lipiodol. Conversely, the observed uniform and stable signal in the radiolipiodol prepared by SHIFT indicates that the radionuclides are uniformly distributed and remain in a stable state over an extended period. Subsequently, the release behavior of radionuclides from the radiolipiodol *in vitro* was also studied using saline as the extractant. The results indicated that the release rates of ^{131}I and ^{177}Lu in ^{131}I-LUF(M) and ^{177}Lu-LUF(M); respectively reached more than 50% in a short interval of time, while the radionuclides in the ^{131}I-LUF(S) and ^{177}Lu-LUF(S) did not release significantly with a release rate of approximately 5% (Fig. 1D). The above-mentioned *in vitro* studies exhibit that the radiolipiodol obtained by SHIFT has splendid stability and uniformity, which can avoid the erosion of radionuclides under the condition of physical coating. Besides, the combination of lipiodol and radionuclides may also exhibit a synergistic effect, the incorporation of lipiodol as a medium may enhance the Cerenkov effect of radionuclides due to the higher refractive index compared to water, serum, and other media. The results of ^{18}F in pure water and lipiodol revealed that the Cerenkov effect was enhanced in ^{18}F-LUF(M) in comparison with free ^{18}F in water. Moreover, enhanced Cherenkov luminescence of ^{18}F-LUF(S) prepared by

SHIFT was observed (Supporting Information Fig. S3). The improved stability and uniformity favored by SHIFT may contribute to this enhancement, warranting further investigation.

3.2. *In vivo stability of radiolipiodol in mouse subcutaneous tumor model*

To observe the metabolism of radiolipiodol prepared by SHIFT in the specific physiological tumor-microenvironment, a subcutaneously HCC induced mouse model was established and radiolipiodol encapsulating ^{177}Lu was used as a diagnostic agent. The distribution of the radionuclides in the body was studied by SPECT scanning at different time points after intratumoral injection with the same dose of ^{177}Lu-LUF(M) and ^{177}Lu-LUF(S) (Fig. 2A and B). The ^{177}Lu uptake signal can be observed at the tumor site but also in the spine of the mice after injection of ^{177}Lu-LUF(M), which implies that ^{177}Lu in ^{177}Lu-LUF(M) is unstable and released from the injected tumor. In contrast, a bright signal was observed throughout the injected tumor area more than 2 weeks without signal in the spine or other areas of the body in the mice injected with ^{177}Lu-LUF(S), indicating ^{177}Lu was stable within ^{177}Lu-LUF(S) and highly enriched within tumors. The radionuclide content in the blood of the mice was also analyzed to explore the metabolism of radionuclides (Fig. 2C). The results showed that ^{177}Lu metabolized gradually and reached the peak at 6 h after injection of ^{177}Lu-LUF (M). Whereas, ^{177}Lu had a maximum blood level of no more than 1% ID/g and maintained at long-term low concentrations after the injection of ^{177}Lu-LUF(S). Thus, it can be seen that ^{177}Lu can enter the blood after rapidly being released from ^{177}Lu-LUF(M), but not from ^{177}Lu-LUF(S), which is consistent with the results of SPECT imaging. Furthermore, massive radionuclide leakage occurred only at 2 h after intratumoral injection of ^{18}F-LUF(M) and was enriched in the spine (Supporting Information Fig. S4). On the 7th day after the injection of radiolipiodol, tumors and major organs were collected for biodistribution analysis (Fig. 2D). According to the value of % ID/g in each tissue, although ^{177}Lu-LUF(M) had a high retention in the tumor, there was still a high radionuclide enrichment in the bone due to the diffusion of ^{177}Lu. On the contrary, the majority of ^{177}Lu in ^{177}Lu-LUF(S) was retained in tumors, and the relative content of ^{177}Lu in^{177}Lu-LUF(S) was more than 5 times than that in ^{177}Lu-LUF(M). The relative ratio of tumor to normal tissue (*T/N*) in ^{177}Lu-LUF(S) could reach hundreds or more (Fig. 2E). These results demonstrate that ^{177}Lu-LUF(S) has prominent intratumoral stability and retention and can provide high contrast dose for local irradiation of tumors, while avoiding unnecessary irradiation burden on normal tissues caused by off-labeling radionuclide.

3.3. *In vivo stability of radiolipiodol in rat orthotopic liver cancer model*

Lipiodol injected by intra-arterial intervention can achieve embolization of the feeding artery and local delivery of drugs for HCC treatment[29]. Therefore, we constructed a rat orthotopic HCC model that was more consistent with the clinical injection method of lipiodol to verify the feasibility of practical application of radiolipiodol[30]. After successful implantation of the orthotopic

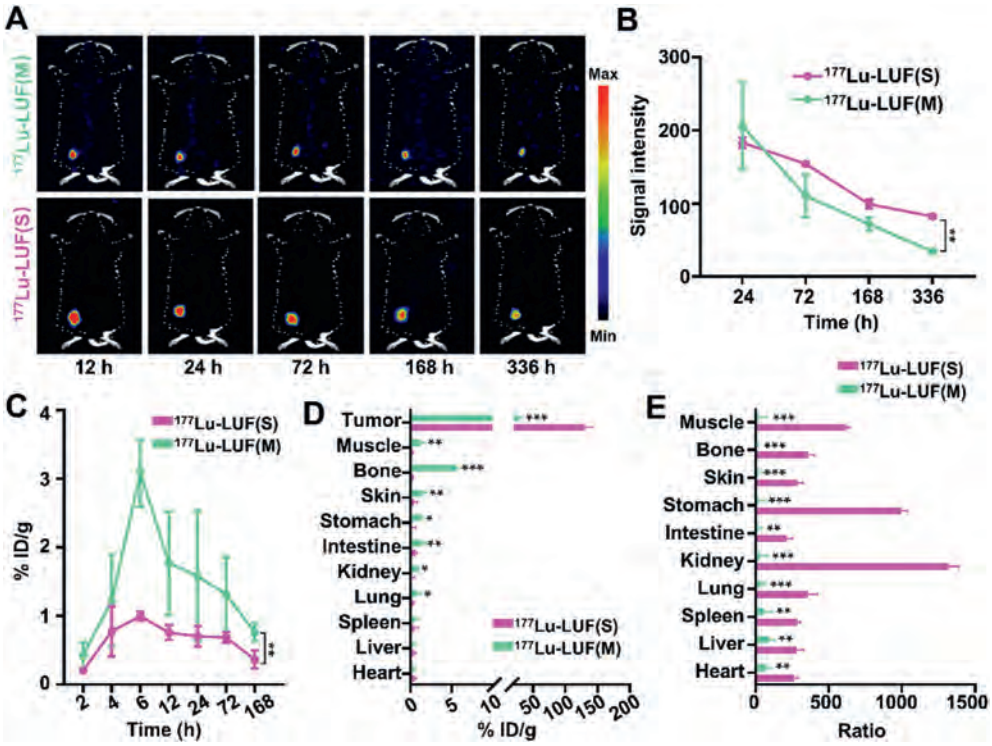

Figure 2 *In vivo* stability studies of radiolipiodol in mouse subcutaneous tumor model. (A) SPECT images of mice following intratumoral injection of ^{177}Lu-LUF. (B) The quantification of the tumor region's ^{177}Lu signal intensity during SPECT monitoring intervals. (C) Blood metabolic curve of mice administered intratumorally with ^{177}Lu-LUF. (D) The biodistribution of ^{177}Lu-LUF in mice following intratumoral injection. (E) Ratio of radionuclide uptake in tumor to normal tissues (*T/N*). Data are presented as mean ± SD ($n = 3$). $^{*}P < 0.05$, $^{**}P < 0.01$, $^{***}P < 0.001$ were considered as significant statistical differences.

HCC rats model[31], the radiolipiodol was injected slowly from the duodenal artery to the proper hepatic artery, and the rats were scanned by SPECT-CT to observe the distribution of radiolipiodol in the whole body, and the locoregional treatment of radiolipiodol might contribute to the superstable radionuclide's retention (Fig. 3A). To confirm the success of hepatic artery embolization, CT imaging was conducted, and obvious signals could be observed in the orthotopic liver tumor, indicating that the injected radiolipiodol was successfully deposited in the tumor location. Besides, the radionuclide signal was mainly present in the liver without altered distribution after ^{177}Lu-LUF(S) injection, while the SPECT signal showed diffusion in the liver and other normal parts after ^{177}Lu-LUF(M) injection (Fig. 3B). Moreover, the SPECT signal of ^{177}Lu-LUF(S) in the tumor area could be maintained for more than a week, indicating that ^{177}Lu-LUF(S) was always in the tumor area, and there were few dissociations of ^{177}Lu (Fig. 3C).

The results of blood metabolism test revealed that ^{177}Lu-LUF(M) is also unstable *in vivo* after arterial injection, which can allow it to quickly enter in the bloodstream. The content of ^{177}Lu in the blood of rats reached the peak at 6−12 h after injection of ^{177}Lu-LUF(M), while the blood level of ^{177}Lu was maintained at a low level of less than 3%ID/g after ^{177}Lu-LUF(S) injection (Fig. 3D). Biodistribution results display that the content of ^{177}Lu is relatively less in tumors but higher in bone and liver in the ^{177}Lu-LUF(M) group. On the contrary, the amount of ^{177}Lu in tumor tissues injected with ^{177}Lu-LUF(S) is up to 20%ID/g, which was more than 4 times that in the ^{177}Lu-LUF(M) group. In addition, there was little distribution of ^{177}Lu in other normal tissues after ^{177}Lu-LUF(S) injection, especially in bones where free ^{177}Lu was good at aggregation (Fig. 3E). The examination of the signal-to-noise ratio (SNR) in SPECT imaging of tumor and other normal tissues indicated ^{177}Lu-LUF(S) had a remarkable increased SNR value than ^{177}Lu-LUF(M), and the ^{177}Lu-LUF(S) group's tumor tissue to liver and bone content ratio was up to ten times higher, demonstrating that ^{177}Lu of ^{177}Lu-LUF(S) was favorably retained in the tumor tissue than ^{177}Lu-LUF(M) (Fig. 3F). The above-mentioned results indicate that ^{177}Lu-LUF(S) can stably accumulate in the tumor area without distinct leakage and uniform metabolism of ^{177}Lu in rat orthotopic HCC model, even if the injection method is non-superselective. To further validate the universality of SHIFT for radiolipiodol, ^{64}Cu-based radiolipiodol prepared by SHIFT was further evaluated for *in vivo* radionuclide distribution. Following interventional administration, the radionuclides in the conventional mixed ^{64}Cu-LUF(M) group exhibited a diffuse distribution throughout the liver and a broad systemic presence. In contrast, PET imaging of the SHIFT-prepared ^{64}Cu-LUF(S) revealed that, while some radionuclide metabolism was observed in the liver and kidneys, the majority of the radionuclides remained localized in the region of transarterial embolization (Supporting Information Fig. S5). This further demonstrates that the application of SHIFT for TARE can be extended to other radionuclides.

3.4. *In vivo stability of radiolipiodol in rabbit orthotopic liver cancer model*

Through the stability studies on two small animals, it has been basically confirmed that the radiolipiodol prepared by SHIFT has distinguished stability in tumors. Subsequently, we verified the

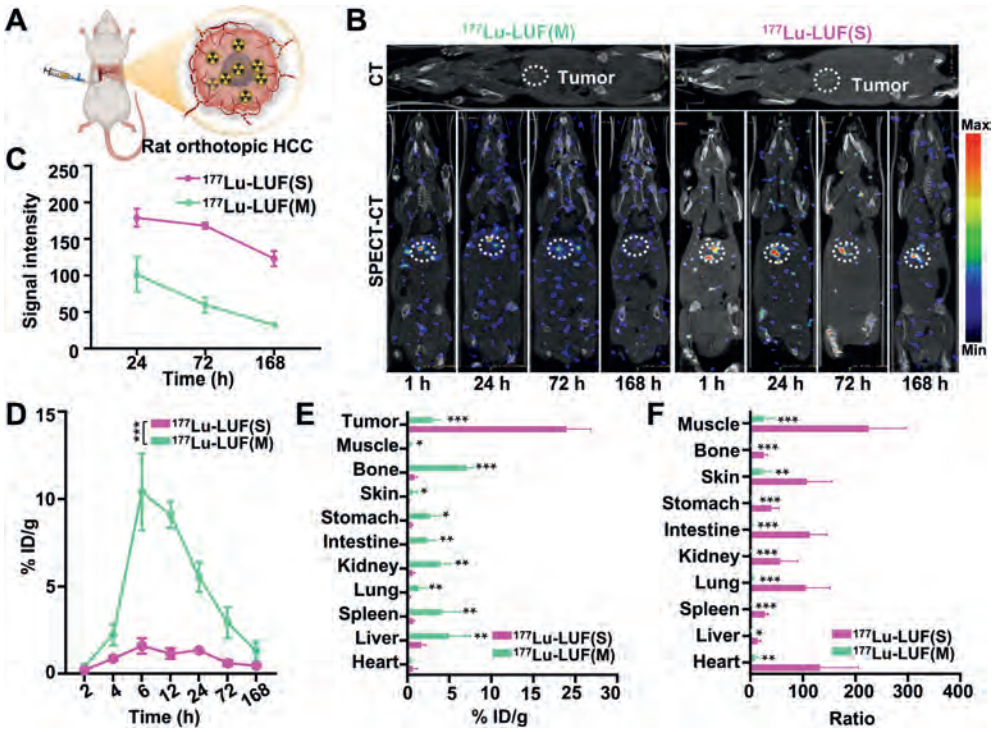

Figure 3 *In vivo* stability studies of radiolipiodol in rat orthotopic liver tumor model. (A) Schematic diagram of the validation of radiolipiodol as a superstable embolic agent to achieve long-term radionuclide tumor enrichment in a rat orthotopic HCC model. (B)SPECT imaging of rats following intraarterial injection of ^{177}Lu-LUF. (C) Signal change curve of the tumor location in the SPECT scanning images subsequent to Radiolipiodol administration. (D) Metabolism profile of ^{177}Lu in rat blood following arterial injection of ^{177}Lu-LUF. (E) Biodistribution of rats with intraarterial injection of ^{177}Lu-LUF. (F) Ratio of radionuclide uptake in tumor tissue to organs. Data are presented as mean ± SD ($n = 3$). $^{*}P < 0.05$, $^{**}P < 0.01$, $^{***}P < 0.001$ were considered as significant statistical differences.

stability of radiolipiodol in a large animal model, namely VX2 rabbit orthotopic HCC model, in order to lay the foundation for clinical application[32]. Interventional injection of radiolipiodol was performed using a microcatheter under the guidance of DSA, and SPECT-CT scans were performed on the 5th and 10th days post-administration. The accumulation of radiolipiodol in the tumor blood vessels can be observed by intraoperative DSA angiography, indicating that the lipiodol treated by SHIFT still retains the siphon effect on the tumor, which is conducive to the realization of local tumor radiotherapy (Supporting Information Fig. S6). SPECT images revealed that the ^{177}Lu signals were distributed throughout the body, among which most enriched in the spine and joint cavity, while a weak signal was observed in the liver on the 5th day after intervention with ^{177}Lu-LUF(M) (Fig. 4A). Particularly, SPECT signal intensity of the tumor is lower than that of the spine region, and the ratio is close to 1 after 10 days of metabolism. This result indicates that the simple mixture of radiolipiodol in the large animal model still cannot stably retain in the tumor area, and there is a serious accumulation of ^{177}Lu in the spine, which may lead to the inhibition of bone marrow cell activity in the spinal cavity at a therapeutic high dose. As for ^{177}Lu-LUF(S), the SPECT-CT images show that the radionuclide signal is completely consistent with the CT signal of lipiodol, and aggregates in tumor without diffusion to the spine even on the 10th day. Through the quantification of signal intensity, it can be seen that the tumor area always maintained the highest signal intensity, while the liver and spine present low signal (Fig. 4B). On the basis of the tumor-to-normal tissues (liver and spinal) signal ratios, the signal ratios of ^{177}Lu-LUF(S) group were significantly higher than that of ^{177}Lu-LUF(M) group (Fig. 4C). The imaging results unveil that ^{177}Lu-LUF(S) can better reflect the excellent tumor retention through accurate interventional injection in a large animal orthotopic HCC model.

After interventional administration, blood samples were also collected from the ear vein to detect the blood metabolism in the experimental rabbits (Fig. 4D). The results indicate that rabbit models injected with ^{177}Lu-LuF(M) have a high level of ^{177}Lu in blood on the day of intervention, and it is not completely metabolized until about the fifth day. However, there is low ^{177}Lu content in blood at 10th day after the interventional injection with ^{177}Lu-LUF(S), indicating the off-target release of ^{177}Lu into the blood is inapparent. The biodistribution results on the 5th day after interventional injection showed that rabbits injected with ^{177}Lu-LUF(M) not only had a relatively high distribution in the tumor, but also in the liver and bone (Fig. 4E). On the contrary, the rabbits in the ^{177}Lu-LUF(S) group contained the highest ^{177}Lu content in tumor tissues, which was higher than 100%ID/g, while radionuclide distribution is inconspicuous neither in liver nor bone. According to the distribution ratio of tumor tissue to bone and liver (Fig. 4F), the relative ratios of ^{177}Lu-LUF(S) group was more than 20 times than that of ^{177}Lu-LUF(M) group, reflecting a remarkable target tissue uptake behavior. These results indicate that ^{177}Lu-LUF(S) has excellent stability in rabbit orthotopic HCC model without significant radionuclide release to blood and only retained in the injected tumor tissue, which lays a persuasive foundation for HCC TARE.

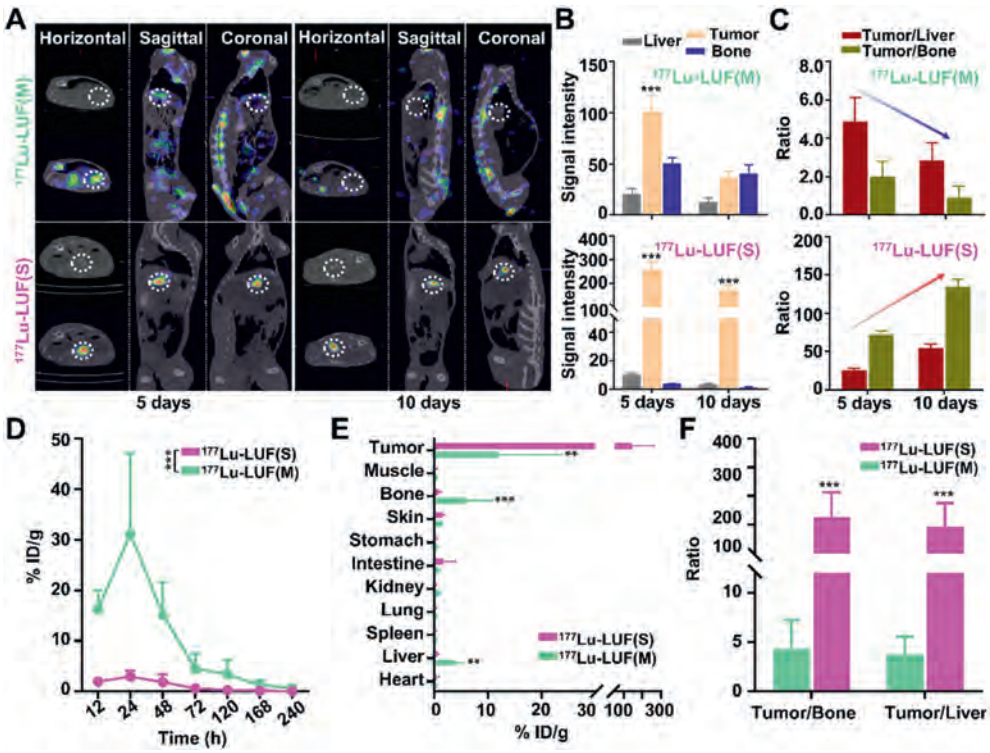

Figure 4 *In vivo* stability studies of ^{177}Lu-LUF in rabbit orthotopic liver cancer model. (A) SPECT imaging of rabbits with transarterial injection of ^{177}Lu-LUF. (B) Signal change curves of tumor, liver and marrow in SPECT images of ^{177}Lu-LUF(M) and ^{177}Lu-LUF(S) groups. (C) Signal intensity ratios of tumor to liver and bone in SPECT images of ^{177}Lu-LUF(M) group and ^{177}Lu-LUF(S) groups. (D) Blood metabolism curve in rabbits injected with ^{177}Lu-LUF intraarterially. (E) Biodistribution of rabbits injected with ^{177}Lu-LUF intraarterially. (F) Ratio of radionuclide uptake in tumor tissue to liver and bone. Data are presented as mean ± SD ($n = 3$). $^{**}P < 0.01$, $^{***}P < 0.001$ were considered as significant statistical differences.

Meanwhile, to further explore the universality of SHIFT technology, we also explored the stability of ^{131}I-based and ^{18}F-based radiolipiodol in rabbit orthotopic HCC model. SPECT-CT imaging exhibit that^{131}I-LUF(S) signal is highly concentrated in the tumor area of the liver, while the radionuclides in ^{131}I-LUF (M) diffuse in the liver and the whole body, and the signals are aggregated in the thyroid on the 5th day after injection because of the specific uptake of iodine by the thyroid gland (Supporting Information Fig. S7A). Through the signal statistics of each part, it can be seen that ^{131}I-LUF(S) presents a signal to noise ratio that is hundreds of times better than that of ^{131}I-LUF(M) (Figs. S7B and S7C). Moreover, the PET-CT scan shows that there is an inapparent signal in the tumor area and well-marked signal in the spine at 2 h after interventional ^{18}F-LUF(M) injection, while there is the opposite signal distribution after ^{18}F-LUF(S) injected (Supporting Information Fig. S8A). Through the signal statistical analysis, it can be observed that ^{18}F-LUF(S) dramatically enriches in the tumor region (Figs. S8B and S8C). These results indicate that ^{131}I-LUF and ^{18}F-LUF prepared by SHIFT both exhibit satisfactory stability and aggregation in the tumor artery, which confirms the feasibility of SHIFT for the application of various types of radionuclides and shows an anticipating prospect for clinical application.

3.5. Stability of radiolipiodol in clinical trial

In the above study, we confirmed that the ultra-stable radiolipiodol prepared by SHIFT has outstanding encapsulating efficiency and stability. Subsequently, the accumulation and stability of radiolipiodol in tumors were verified in various dynamic animal models such as mouse subcutaneous tumor model, rat and rabbit orthotopic HCC model, and especially the feasibility of its application in interventional embolization and radiotherapy for HCC was confirmed. Studies reported that low-dose radionuclides used for diagnostic purposes have immunomodulatory effects, which may potentially improve cancer treatment[33]. Based on the satisfactory results of preclinical studies, an exploratory clinical trial was conducted to observe whether the radiolipiodol prepared by SHIFT could maintain excellent manifestation in the scenario and improve the curative effect of clinical application. In order to reduce the superfluous irradiation to patients, the stability of ^{18}F-LUF as a representative diagnostic agent was observed in this study, to lay down the foundation for the further applications of therapeutic radionuclides.

We first screened a 65-year-old man with HCC according to inclusion criteria. The results of abdominal MRI plain scan and enhanced contrast scan showed that there were about 2.0 cm × 2.4 cm × 2.6 cm and 1.0 cm × 0.8 cm × 0.9 cm lesions in the right posterior lobe and the right anterior lobe of the liver, respectively (Fig. 5A and B). At the time of surgery, the angiographic findings are shown in Fig. 5C. Nodular abnormal tumor staining foci with well-defined boundaries and regular shapes were seen in the liver, which was supplied by branches of the right hepatic artery, and the tumor-feeding arteries were tortuous and disordered. The right portal vein showed early in the arterial phase, which was considered as a hepatic artery-portal vein fistula. The main trunk and branches of the portal vein were well displayed, and no exact filling defect was found. According to the protocol, saline 100 mL and fluorouridine 0.5 g were slowly injected into the common hepatic artery, and a total of 5 mL ^{18}F-LUF and epirubicin 30 mg mixed emulsion were slowly injected into the superselective tumor feeding artery through a microcatheter for TACE, and then gelatin sponge particles were used to supplement the embolization of tumor hepatic artery-portal vein fistula. The angiographic review showed desired deposition of lipiodol, disappearance of tumor staining as well as most of the hepatic artery-portal fistula.

The patients were sent to the nuclear medicine department for PET-CT scanning immediately, and the distribution of ^{18}F-LUF in the body was observed at 0.5 h after the intervention. As shown in Fig. 5D, arresting ^{18}F signals are observed in the tumor, liver, kidney, and bladder, indicating that ^{18}F-LUF was not completely deposited in the tumor area. The probable reason may be the excessive use of dispersed solvent with chemotherapy drugs leads to the increase of ^{18}F-LUF mobility, and the existence of hepatic artery-portal vein fistula in the patient's lesion, eventually leading to more loss of ^{18}F-LUF. The CT scan of the upper and middle abdomen was performed on the 21st day after TACE (Fig. 5E). The results showed no abnormality in the size and shape of the liver, with a nodular slightly low-density shadow about 2.3 cm × 2.1 cm in size. A small amount of lipiodol was distributed in the tumor and the surrounding liver tissue, but it was mainly retained in the tumor area. MRI scan was performed 66th day after the intervention (Supporting Information Fig. S9), and the nodular abnormal signal shadow was seen in the right posterior lobe of the liver, with a large range of about 2.0 cm × 2.1 cm. The lesions in the right posterior lobe of the liver were mainly necrotic, indicating a good prognosis after treatment. In addition, no obvious abnormalities were found in the postoperative liver function serum indexes and blood routine tests (Supporting Information Figs. S10A−S10D), which suggests the safety of ^{18}F-LUF and SHIFT strategy *in vivo*. And the significant decrease in alpha-fetoprotein, suggesting the efficacy of the embolization (Fig. S10E). In this case, excessive solvent and the patient's arteriovenous fistula led to the uncorking of ^{18}F to the non-injection area. Although the patient achieved a good response that may be due to the effect of immune response stimulated by low-dose radionuclides[33], it did not truly reflect the stability of ^{18}F-LUF in the tumor.

Based on the experience of case 1, we then optimized the dispensing regimen and selected patients with typical diagnostic features to conduct the trial again. The MRI examination of case 2 showed a mass of abnormal signal shadow in the right anterior lobe of the liver, the size was about 6.3 cm × 5.2 cm (Fig. 6A and B), and was diagnosed as primary HCC. At the time of interventional procedures, angiography showed a mass of abnormal tumor staining in the liver with clear boundaries and regular shapes (Fig. 6C). The blood supply was from multiple branches of the right hepatic artery, and the tumor-feeding artery was tortuous and disordered. The main portal vein and branches were well displayed without definite filling defect shadow. A mixture of 5 mL ^{18}F-LUF and 40 mg epirubicin was slowly injected into each of the tumor-feeding arteries through a microcatheter for TACE, and then the tumor-feeding arteries were embolized with gelatin sponge particles. The re-examination of angiography showed that the ^{18}F-LUF was well deposited and the tumor staining disappeared.

PET-CT scan at 30 min after operation showed that there were obvious CT signals in the tumor area and bladder (Fig. 6D), which were caused by the deposition of injected lipiodol and metabolism of iohexol, the CT contrast agent used in the interventional procedure, respectively. At the same time, the tumor showed a bright PET signal, which was consistent with the lipiodol signal in CT, indicating that ^{18}F-LUF was highly aggregated here. There was also a small amount of signal in the bladder, which was due to the washout metabolism of the intraoperative contrast material for angiography. In addition, there was a feeble signal in the spinal

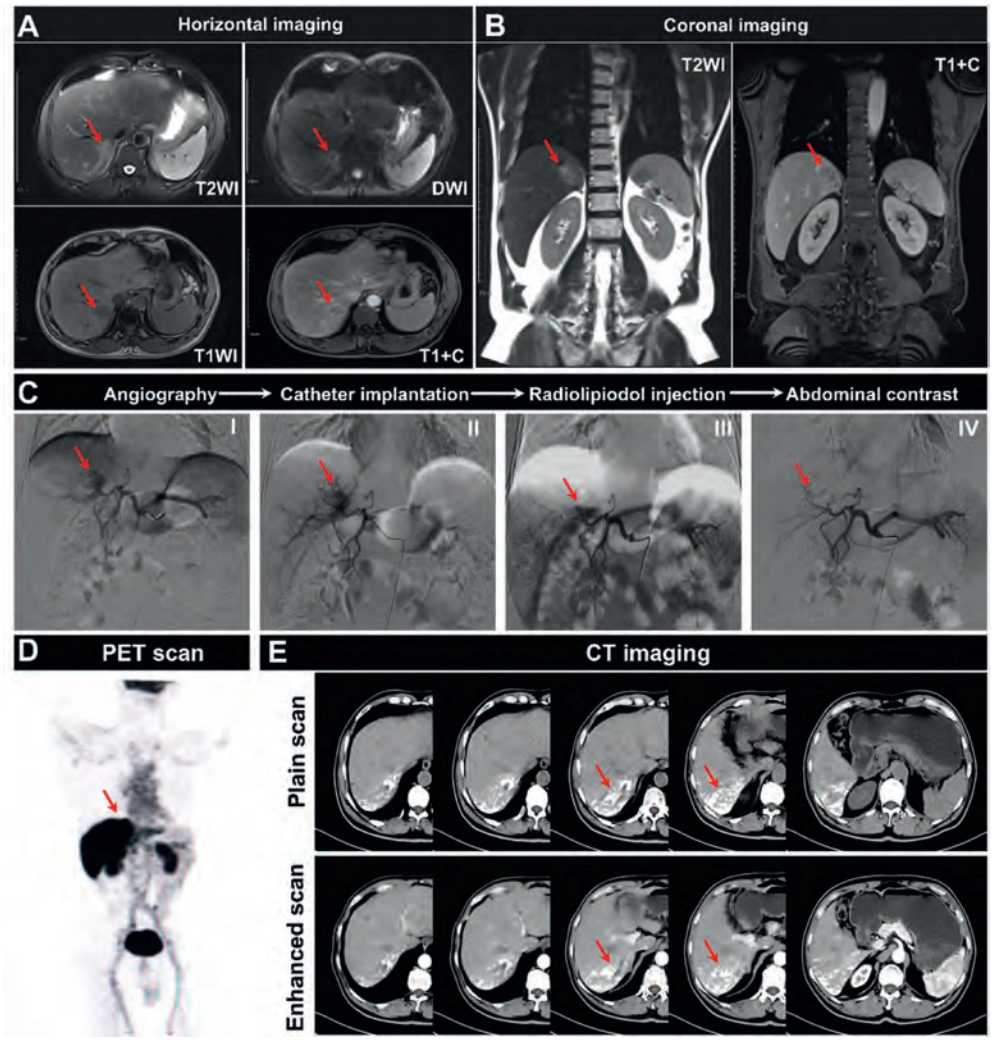

Figure 5 Stability studies of radiolipiodol in case 1 of HCC. (A) MRI horizontal plane image of case 1. (B) MRI coronal image of case 1, the red arrow indicated the lesion area of the liver cancer. (C) DSA-guided hepatic artery embolization in case 1, including I: tumor angiography, II: the microcatheter traveled to the main tumor feeding artery under the guidance of DSA, III: injection of ^{18}F-LUF(S), and IV: abdominal contrast after ^{18}F-LUF injected, the red arrow indicated the lesion area of the tumor. (D) PET scan of case 1 at 1 h after ^{18}F-LUF injection. (E) CT scan of case 1 on the 21st day after ^{18}F-LUF injection.

region and other tissues of the liver, showing minimal loss of ^{18}F metabolism. A repeated PET-CT scan at 180 min after surgery also showed a hyperintense signal in the tumor area, while the signal in other tissues was negligible. Statistical analysis of PET and CT signal intensity further demonstrated that ^{18}F-LUF was highly enriched in tumors and exhibited an admirable signal-to-noise ratio (Fig. 6E). Furthermore, on post-operative serologic examination, there was no abnormal liver function, suggesting the safety of the SHIFT-based radiolipiodol (Supporting Information Fig. S11). This study confirmed the stability and feasibility of radiolipiodol prepared by SHIFT in clinical interventional therapy, and laid a reliable research foundation for the subsequent therapeutic application.

4. Discussion

TARE based radionuclide for HCC was widely used in clinical practice decades ago[34]. However, the clinical application of radiolipiodol has gradually decreased because of the adverse reactions, the limited efficacy and the application conditions[35]. In this study, we expanded the application of SHIFT dispensing technology in the field of nuclear medicine, and provided a new technical reference for improving the preparation methods of radiolipiodol and optimizing its effect in clinical applications. We first explored the application of SHIFT in the preparation of radiolipiodol based on ^{177}Lu, ^{131}I and ^{18}F to obtain considerable yield and specific activity preparations. Radiolipiodol obtained by SHIFT had more than 99% encapsulating efficiency, homogeneous distribution of radionuclides in the lipiodol, and excellent *in vitro* stability. In a mouse subcutaneous tumor model of HCC, ^{177}Lu-LUF(S) was injected into the tumor area by intratumoral injection. SPECT imaging, blood metabolism analysis and biodistribution detection were used to verify the brilliant accumulation of ^{177}Lu in radiolipiodol in the tumor, and there was no leakage of ^{177}Lu into the blood and uptake in normal tissues. It was also observed that ^{177}Lu-LUF(S), ^{131}I-LUF(S) and ^{18}F-LUF(S) absolutely aggregated in orthotopic HCC after

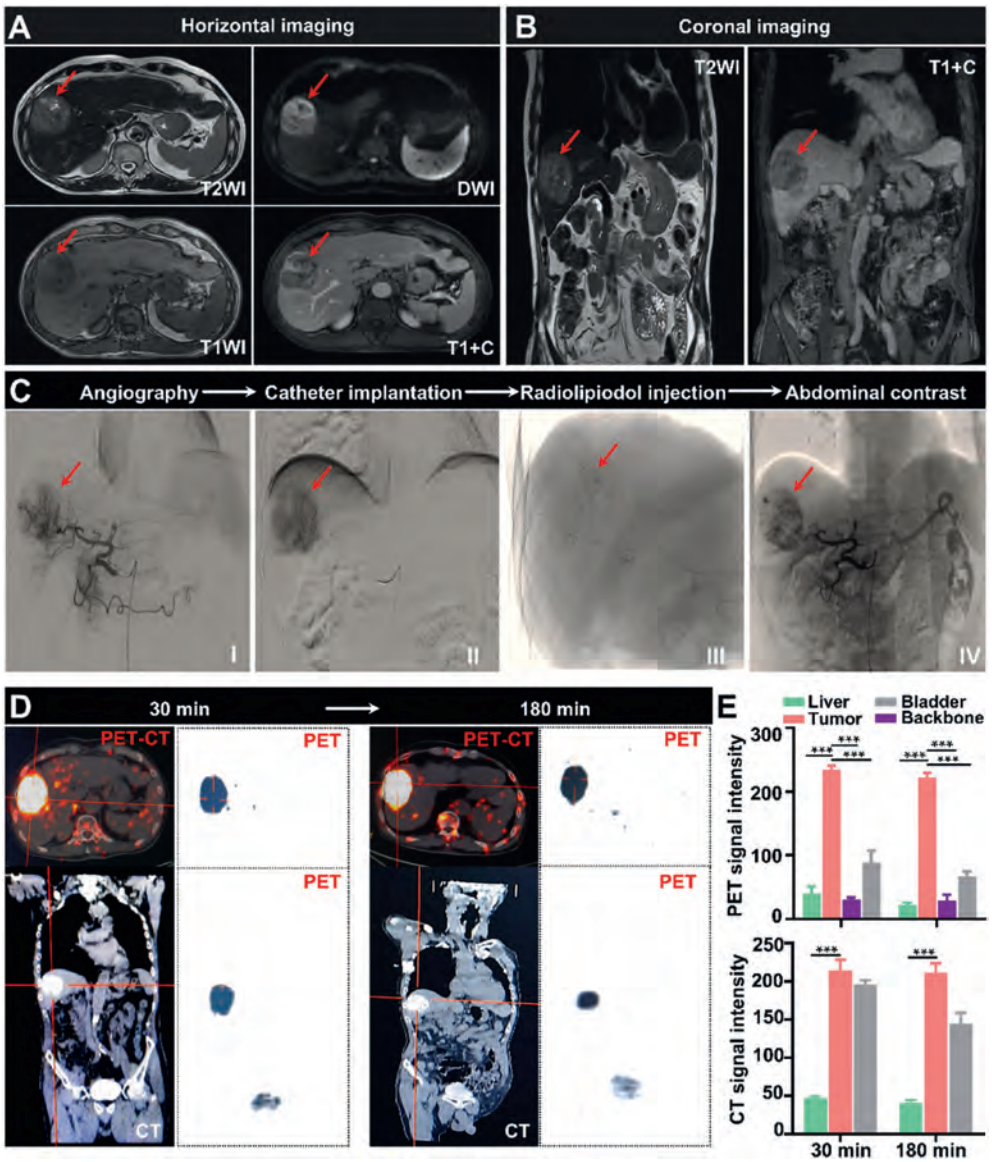

Figure 6 Feasibility analysis of radiolipiodol in interventional therapy of case 2 of HCC. (A, B) MRI images at diagnosis in case 2, including the horizontal plane image and the coronal plane image. The red arrow indicated the lesion area of tumor. (C) In case 2, DSA-guided hepatic artery embolization involved (I) tumor angiography, (II) microcatheter guidance to the major tumor feeding artery, (III) injection of ^{18}F-LUF(S), and (IV) abdominal contrast following injection, the red arrow indicated the lesion area of tumor. (D) PET-CT image of case 2 after interventional injection with ^{18}F-LUF(S). (E) Quantitative analysis of signal intensity in liver, tumor, bladder and backbone using region of interest (ROI) from the PET and CT images, and ROI values are presented as mean ± SD. ***$P < 0.001$ were considered as significant statistical differences.

interventional injection through the hepatic artery without ectopic loss. Through the above preclinical systematic studies, we confirmed the stability, reliability and feasibility of radiolipiodol prepared by SHIFT for the diagnosis and treatment of HCC *in vitro* and *in vivo*.

Based on the promising results of preclinical study, we are encouraged to move SHIFT into clinical trials. After the approval of the ethics committee in the Affiliated Hospital of North Sichuan Medical College, we carried out clinical validation in strict accordance with the trial protocol and relevant regulations through the coordination and cooperation of multiple departments in the hospital. This clinical trial was an exploratory trial to observe whether the radiolipiodol prepared by SHIFT could maintain stable enrichment in the lesions, and whether there was metabolism and detachment of radionuclides after injection into the HCC area by means of intervention. In addition, the introduction of low-dose radionuclides also has the value of potentially improving the therapeutic effect of cancer by regulating the immune microenvironment[33]. In the first clinical study, due to the excessive use of solvent during the mixture of chemotherapy drugs and the existence of arteriovenous fistula in the patient's lesion, ^{18}F was hyperintense in the non-injected area. Although the patient achieved a considerable curative response, it did not truly reflect the stability of ^{18}F-LUF in the tumor. On the basis of experience with this trial, we then selected another patient with more desirable diagnostic features and performed the trial again.

In case 2 study, after optimizing the formulation method and avoiding the arteriovenous fistula, ^{18}F-LUF markedly enriched in the tumor and exhibited a terrific signal-noise ratio (SNR), as observed by PET-CT imaging. In addition, the patient's blood and serological tests showed no significant adverse reactions. Collectively, the above studies confirmed the stability and feasibility of radiolipiodol prepared by SHIFT for HCC endovascular intervention, and laid a persuasive research foundation for the subsequent therapeutic application.

5. Conclusions

This study introduces a novel radiolipiodol formulation using SHIFT in a carbon dioxide supercritical fluid environment. This technique encapsulates radionuclides into lipiodol, avoiding the complexities of traditional chemical labeling methods. The resulting radiolipiodol demonstrates exceptional stability and ultra-high labeling efficiency with no significant radionuclide leakage. The preclinical models and clinical trials show notable intratumoral radionuclide retention and minimal leakage. SHIFT presents a reliable and efficient strategy for radionuclide encapsulation, offering significant promise for enhancing TARE in HCC, paving the way for improved clinical applications.

Acknowledgments

This work was supported by the Major State Basic Research Development Program of China (No. 2023YFB3810000), the National Natural Science Foundation of China (NSFC) (Nos. 82402501, 81925019, 81801817, 82360360, U22A20333 and U24A20525), Natural Science Foundation of Guangxi (No. 2023GXNSFAA026023, China), Central Government Guided Local Science and Technology Development Fund Projects (No. 2023ZYZX1090, China), Nanchong Science and Technology Bureau basic research platform project (No. 23JCYJPT0043, China), China Postdoctoral Science Foundation, (Nos. 2023MD734156 and 2024M763915). The home-for-researchers website contributed to literature review and writing.

Author contributions

Hu Chen, Hongwei Cheng and Gang Liu designed the research. Hu Chen, Yongfu Xiong, Minglei Teng, Yesen Li, Suping Li and Jingsong Mao carried out the experiments and performed data analysis. Deliang Zhang, Yongjun Ren, Zheng Li, Hui Liu and Jinxiong Huang participated part of the experiments. Xiaofei Wen, Zhenjie Li and Rongqiang Zhuang provided experimental drugs and quality control. Hu Chen wrote the manuscript. Yang Zhang, Syed Faheem Askari Rizvi, Hongwei Cheng and Gang Liu revised the manuscript. All of the authors have read and approved the final manuscript.

Conflicts of interest

The authors have no conflicts of interest to declare.

Appendix A. Supplementary information

Supporting information to this article can be found online at https://doi.org/10.1016/j.apsb.2025.02.021.

References

1. Gordan JD, Kennedy EB, Abou-Alfa GK, Beal E, Finn RS, Gade TP, et al. Systemic therapy for advanced hepatocellular carcinoma: ASCO guideline update. *J Clin Oncol* 2024;**42**:1830−50.
2. Johnson P, Zhou Q, Dao DY, Lo YMD. Circulating biomarkers in the diagnosis and management of hepatocellular carcinoma. *Nat Rev Gastroenterol Hepatol* 2022;**19**:670−81.
3. Scott AM, Zeglis BM, Lapi SE, Scott PJH, Windhorst AD, Abdel-Wahab M, et al. Trends in nuclear medicine and the radiopharmaceutical sciences in oncology: workforce challenges and training in the age of theranostics. *Lancet Oncol* 2024;**25**:e250−9.
4. Teng ML, Liang XL, Liu H, Li ZJ, Gao X, Zhang C, et al. Cerenkov radiation shining a light for cancer theranostics. *Nano Today* 2024;**55**: 102174.
5. Salem R, Johnson GE, Kim E, Riaz A, Bishay V, Boucher E, et al. Yttrium-90 radioembolization for the treatment of solitary, unresectable HCC: the LEGACY study. *Hepatology* 2021;**74**:2342−52.
6. Raoul JL, Boucher E, Rolland Y, Garin E. Treatment of hepatocellular carcinoma with intra-arterial injection of radionuclides. *Nat Rev Gastroenterol Hepatol* 2010;**7**:41−9.
7. Salem R, Mazzaferro V, Sangro B. Yttrium 90 radioembolization for the treatment of hepatocellular carcinoma: biological lessons, current challenges, and clinical perspectives. *Hepatology* 2013;**58**:2188−97.
8. Prince JF, van Rooij R, Bol GH, de Jong HW, van den Bosch MA, Lam MG. Safety of a scout dose preceding hepatic radioembolization with 166Ho microspheres. *J Nucl Med* 2015;**56**:817−23.
9. Xu X, Chen H, Zhao ZW, Wang YJ, He P, Cheng HW, et al. Engineering radioactive microspheres for intra-arterial brachytherapy using radiation-induced graft polymerization. *Adv Funct Mater* 2023;**33**: 2306215.
10. Xu X, Chen H, He P, Zhao ZW, Gao X, Liu C, et al. 3D hollow porous radio-granular hydrogels for SPECT imaging-guided cancer intravascular brachytherapy. *Adv Funct Mater* 2023;**33**:2215110.
11. Qian YY, Liu QF, Li PL, Han YB, Zhang JP, Xu JJ, et al. Highly Tumor-specific and long-acting iodine-131 microbeads for enhanced treatment of hepatocellular carcinoma with low-dose radio-chemoembolization. *ACS Nano* 2021;**15**:2933−46.
12. Raoul JL, Boucher E, Rolland Y, Garin E. Treatment of hepatocellular carcinoma with intra-arterial injection of radionuclides. *Nat Rev Gastroenterol Hepatol* 2010;**7**:41−9.
13. Pérez-López A, Martín-Sabroso C, Gómez-Lázaro L, Torres-Suárez AI, Aparicio-Blanco J. Embolization therapy with microspheres for the treatment of liver cancer: state-of-the-art of clinical translation. *Acta Biomater* 2022;**149**:1−15.
14. Jiang QR, Pu XQ, Deng CF, Wang W, Liu Z, Xie R, et al. Microfluidic controllable preparation of iodine-131-labeled microspheres for radioembolization therapy of liver tumors. *Adv Healthc Mater* 2023;**12**: e2300873.
15. De La Vega JC, Esquinas PL, Rodríguez-Rodríguez C, Bokharaei M, Moskalev I, Liu D, et al. Radioembolization of hepatocellular carcinoma with built-in dosimetry: first *in vivo* results with uniformly-sized, biodegradable microspheres labeled with ^{188}Re. *Theranostics* 2019;**9**:868−83.
16. Leung WT, Lau WY, Ho S, Chan M, Leung N, Lin J, et al. Selective internal radiation therapy with intra-arterial iodine-131-lipiodol in inoperable hepatocellular carcinoma. *J Nucl Med* 1994;**35**:1313−8.
17. Raoul JL, Guyader D, Bretagne JF, Heautot JF, Duvauferrier R, Bourguet P, et al. Prospective randomized trial of chemoembolization *versus* intra-arterial injection of ^{131}I-labeled-iodized oil in the treatment of hepatocellular carcinoma. *Hepatology* 1997;**26**:1156−61.
18. Borbath I, Lhommel R, Bittich L, Goffette P, Annet L, Van Beers BE, et al. ^{131}I-labelled-iodized oil for palliative treatment of hepatocellular carcinoma. *Eur J Gastroenterol Hepatol* 2005;**17**:905−10.
19. Jouneau S, Vauléon E, Caulet-Maugendre S, Polard E, Volatron AC, Meunier C, et al. ^{131}I-labeled lipiodol-induced interstitial pneumonia: a series of 15 cases. *Chest* 2011;**139**:1463−9.

20. Subramanian S, Das T, Chakraborty S, Sarma HD, Banerjee S, Samuel G, et al. Preparation of ^{177}Lu-Labeled oxine in lipiodol as a possible agent for therapy of hepatocellular carcinoma: a preliminary animal study. *Cancer Biother Radiopharm* 2010;**25**:539−43.
21. Cheng HW, Yang XM, Liu G. Superstable Homogeneous iodinated formulation technology: revolutionizing transcatheter arterial chemoembolization. *Sci Bull (Beijing)* 2020;**65**:1685−7.
22. Chen H, Cheng HW, Dai QX, Cheng Y, Zhang Y, Li DF, et al. A superstable homogeneous lipiodol-ICG formulation for locoregional hepatocellular carcinoma treatment. *J Control Release* 2020;**323**: 635−43.
23. Zhang Y, Cheng HW, Chen H, Xu PY, Ren E, Jiang YH, et al. A pure nanoICG-based homogeneous lipiodol formulation: toward precise surgical navigation of primary liver cancer after long-term transcatheter arterial embolization. *Eur J Nucl Med Mol Imaging* 2022;**49**: 2605−17.
24. He P, Xiong YF, Ye JF, Chen BQ, Cheng HW, Liu H, et al. A clinical trial of super-stable homogeneous lipiodol-nanoICG formulation-guided precise fluorescent laparoscopic hepatocellular carcinoma resection. *J Nanobiotechnology* 2022;**20**:250.
25. He P, Xiong YF, Luo B, Liu JM, Zhang Y, Xiong Y, et al. An exploratory human study of superstable homogeneous lipiodol-indocyanine green formulation for precise surgical navigation in liver cancer. *Bioeng Transl Med* 2022;**8**:e10404.
26. Xiong YF, He P, Zhang Y, Chen H, Peng Y, He P, et al. Superstable homogeneous lipiodol-ICG formulation: initial feasibility and first-inhhuman clinical application for ruptured hepatocellular carcinoma. *Regen Biomater* 2023;**10**:rbac106.
27. Mukherjee A, Subramanian S, Ambade R, Avhad B, Dash A, Korde A. Development of semiautomated module for preparation of ^{131}I labeled lipiodol for liver cancer therapy. *Cancer Biother Radiopharm* 2017;**32**: 33−7.
28. Shi XX, Xu DZ, Cheng HW, Chu CC, Liu G. Recent advances in interventional fluorescence imaging: toward the precise visualization of transarterial mini-invasive delivery systems. *Acc Mater Res* 2023;**4**: 251−63.
29. Lencioni R, de Baere T, Soulen MC, Rilling WS, Geschwind JF. Lipiodol Transarterial chemoembolization for hepatocellular carcinoma: a systematic review of efficacy and safety data. *Hepatology* 2016;**64**:106−16.
30. Wang CJ, Zhang L, Yang ZJ, Zhao DX, Deng Z, Xu JL, et al. Self-fueling ferroptosis-inducing microreactors based on pH-responsive lipiodol pickering emulsions enable transarterial ferro-embolization therapy. *Natl Sci Rev* 2024;**11**:nwad257.
31. Liang XL, Liu H, Chen H, Peng XQ, Li ZJ, Teng ML, et al. Rhein-based pickering emulsion for hepatocellular carcinoma: shaping the metabolic signaling and immunoactivation in transarterial chemoembolization. *Aggregate* 2024;**5**:e552.
32. Bai S, Chen H, Fu SY, Liu C, Gao X, Li S, et al. Bioinspired tumor calcification-guided early diagnosis and eradication of hepatocellular carcinoma. *Adv Mater* 2024;**36**:2310818.
33. Wen XJ, Shi CR, Zeng XY, Zhao L, Yao LL, Liu ZD, et al. A paradigm of cancer immunotherapy based on 2-[^{18}F]FDG and anti-PD-L1 mAb combination to enhance the antitumor effect. *Clin Cancer Res* 2022;**28**:2923−37.
34. Mulcahy MF, Mahvash A, Pracht M, Montazeri AH, Bandula S, Martin 2nd RCG, et al. Radioembolization with chemotherapy for colorectal liver metastases: a randomized, open-label, international, multicenter, phase III trial. *J Clin Oncol* 2021;**39**:3897−907.
35. Boucher E, Bouguen G, Garin E, Guillygomarch A, Boudjema K, Raoul JL. Adjuvant intraarterial injection of ^{131}I-labeled lipiodol after resection of hepatocellular carcinoma: progress report of a case-control study with a 5-year minimal follow-up. *J Nucl Med* 2008; **49**:362−6.